Title: Emulating constant acceleration locomotion mechanics on a treadmill

Author: Dominic James Farris[1, 2]

[1]School of Human Movement and Nutrition Sciences, The University of Queensland, Brisbane, Australia

[2]Movement Science, The Australian Institute of Sport, Canberra, Australia.

Corresponding Author: Dominic James Farris, School of Human Movement and Nutrition Sciences, Building 26B, Blair Drive, The University of Queensland, Brisbane, QLD 4072, Australia. Email: d.farris@uq.edu.au, Tel: +61 07 3365 6097, Fax: +61 07 3365 6877.

Keywords: Mechanical work, impulse, walking, running, gait, force

Word Count: 3495

Abstract

Locomotion on an accelerating treadmill belt is not dynamically similar to overground acceleration. The purpose of this study was to test if providing an external force to compensate for inertial forces during locomotion on an accelerating treadmill belt could induce locomotor dynamics similar to real accelerations. Nine males (mean ± sd age = 26 ± 4 years, mass = 81 ± 9 kg, height = 1.8 ± 0.05 m) began walking and transitioned to running on an accelerating instrumented treadmill belt at three accelerations (0.27 $m \cdot s^{-2}$, 0.42 $m \cdot s^{-2}$, 0.76 $m \cdot s^{-2}$). Half the trials were typical treadmill locomotion (TT) and half were emulated acceleration (EA), where elastic tubing harnessed to the participant provided a horizontal force equal to mass multiplied by acceleration. Net mechanical work (W_{COM}) and ground reaction force impulses (I_{GRF}) were calculated for individual steps and a linear regression was performed with these experimental measures as independent variables and theoretically derived values of work and impulse as predictor variables. For EA, linear fits were significant for W_{COM} ($y=1.19x + 10.5$, $P<0.001$, $R^2=0.41$) and I_{GRF} ($y=0.95x + 8.1$, $P<0.001$, $R^2=0.3$). For TT, linear fits were not significant and explained virtually no variance for

W_{COM} ($y=0.06x + 1.6$, $P=0.29$, $R^2<0.01$) and I_{GRF} ($y=0.10x + 0.4$, $P=0.06$, $R^2=0.01$). This suggested that the EA condition was a better representation of real acceleration dynamics than TT. Running steps from EA where work and impulse closely matched theoretical values showed similar adaptations to increasing acceleration as have been previously observed overground (forward reorientation of GRF vector without an increase in magnitude or change in spatio-temporal metrics).

Introduction

The mechanics of human locomotion have been studied extensively. It is now relatively commonplace for research and rehabilitation laboratories to combine motion capture systems with instrumented treadmills to readily obtain many consecutive steps or strides of walking or running data. The use of instrumented treadmills as opposed to in ground force plates also facilitates the use of tethered devices such as stationary bodyweight support systems (Donelan and Kram, 1997), robotic testbeds (Caputo and Collins, 2013) and wired measurement systems (e.g. ultrasound imaging platforms). Although treadmills provide a convenient means of collecting data, under some circumstances they do not provide an accurate replication of overground locomotion dynamics.

Van Ingen Schenau (1980) provided a detailed proof that the dynamics of locomotion on a treadmill with constant belt speed are dynamically similar to constant speed locomotion overground when considered in a reference frame that moves with the belt. However, theoretical and experimental evidence shows that locomotion on an accelerating treadmill belt is not dynamically similar to

41 accelerating overground (Christensen et al., 2000; Van Caekenberghe et al.,
42 2013b). Perhaps the simplest explanation for this is that the person on an
43 accelerating treadmill belt is not actually accelerating in a fixed inertial reference
44 frame, unlike a person accelerating overground. It is also the case that the
45 previously noted reference frame that is attached to the belt is accelerating
46 relative to the world and is considered a non-inertial reference frame. When the
47 belt is accelerated, it causes an inertial force to act upon the user that is opposite
48 in direction to the acceleration and equal to the users mass multiplied by the
49 acceleration of the belt. This force effectively accelerates the user in the belt
50 frame of reference and the user does not have to actively generate propulsive
51 horizontal ground reaction forces to accelerate their body, as they would have to
52 overground. As a result, the mechanics of running on an accelerating treadmill
53 belt have been experimentally shown to be fundamentally different from those
54 for accelerative running overground (Van Caekenberghe et al., 2013b). Therefore
55 it is not appropriate to study accelerative locomotion mechanics during normal
56 walking and running on an accelerating treadmill, unless the acceleration is very
57 low (Goldberg et al., 2008; Peterson et al., 2011). This is inconvenient, because

overground studies limit the use of wired/tethered systems; make it hard to control speed and require either many trials or multiple force platforms to obtain multiple steps. Often human locomotion is not at constant speed and so it would be useful to find an appropriate means of studying accelerative locomotion on a treadmill.

Morin et al. (2010) examined accelerations on a torque treadmill where the user drove the belt acceleration and was rigidly tethered to allow an appropriate body posture. However, without controlling the force in the tether and making it proportional to belt acceleration, one cannot accurately reproduce the forces required to overcome body inertia. An approach presented by Christensen et al. (2000), was to compensate for the inertial forces resulting from belt acceleration by applying a proportional horizontal force (mass multiplied by belt acceleration) in the opposite direction via a tether. In their system, the force was feedback controlled according to belt acceleration and the position of the user on the treadmill. However, the purpose of Christensen et al. (2000) was not to examine the mechanics of the user and so they did not report if similar mechanics to those observed overground were induced by this approach.

This study aimed to assess the effects of emulating acceleration by providing a compensatory horizontal force to negate the inertial effect of belt acceleration on treadmill walking and running mechanics. Two hypotheses were proposed: 1) Providing a compensatory force would induce net mechanical work and net impulses more similar to theoretically derived true values than walking and running on a treadmill without a compensatory force. 2) The effects of emulated acceleration on ground reaction forces (GRF) and temporal metrics for running would be the same as have been observed for overground acceleration (Kugler and Janshen, 2010; Van Caekenberghe et al., 2013a; Van Caekenberghe et al., 2013b). Specifically, increasing belt acceleration would cause a more anterior orientation of the GRF vector during running without affecting the magnitude of the vector or step and stance times. To provide proof of concept, a simplified case is presented where belt acceleration is constant, and therefore the inertial and compensatory forces are constant, negating the need for feedback control.

Methods

90 *Participants & protocol* - Nine male participants (mean ± sd age = 26 ± 4 years,
91 mass = 81 ± 9 kg, height = 1.8 ± 0.05 m) gave written informed consent to
92 participate in this study that was approved by an institutional ethics review
93 committee. Each participant initially walked on a split belt instrumented treadmill
94 (DBCEEWI, AMTI, USA) at 0.75 $m \cdot s^{-1}$ and naturally transitioned to a run during a
95 period of treadmill belt acceleration that increased belt speed to 2.75 $m \cdot s^{-1}$. This
96 was repeated four times at each of three accelerations (A1: 0.27 $m \cdot s^{-2}$, A2: 0.42
97 $m \cdot s^{-2}$, A3: 0.76 $m \cdot s^{-2}$) for two experimental conditions (total of 24 trials). One
98 experimental condition was typical treadmill locomotion (TT) and the other was
99 emulated acceleration (EA) where a backward horizontal force was applied to the
100 user via a tensioned rubber spring element attached to a harness worn by the
101 user (Figure 1). For TT, participants also completed constant speed (A0) trials for
102 walking (1.25 $m \cdot s^{-1}$) and running (2.25 $m \cdot s^{-1}$). Comparing the accelerations used
103 with previous studies, they fall within the mid-range for volitional overground
104 running accelerations (Van Caekenberghe et al., 2013b) and the A1 and A2
105 conditions are similar to volitional overground walking accelerations (Qiao and
106 Jindrich, in press).

Emulating acceleration mechanics - The EA condition was intended to induce mechanics (GRF impulse, external net mechanical work) similar to that which would be required for overground accelerations. Ignoring frictional and aerodynamic forces, a person accelerating overground has these dynamics:

$$F_h = ma_g \qquad (1)$$

Where F_h is the net horizontal GRF, m is the person's mass and a_g is the horizontal acceleration of the body in a ground-based fixed reference frame. For typical treadmill locomotion where the belt is accelerated relative to the ground-based reference frame the dynamics can be described by:

$$F_h = ma_{p/b} + ma_{b/g} \qquad (2)$$

Where $a_{p/b}$ is the acceleration of the person in a frame of reference moving with the treadmill belt and $a_{b/g}$ is acceleration of the treadmill belt in the ground-based frame of reference. The term $ma_{b/g}$ represents the inertial force acting on the person as a result of the acceleration of the belt. If the person remains in the same position on the treadmill, then $a_{p/b}$ must be equal and opposite to $a_{b/g}$ and the F_h will equal zero. From equation 1, we see that overground, F_h cannot be

zero if the person is accelerating and therefore typical treadmill locomotion is not dynamically similar to overground. As proposed by Christensen et al. (2000), we can treat the inertial force $ma_{b/g}$ as an external force and apply an opposing horizontal external force to get the following dynamics:

$$F_h - ma_{b/g} + F_{app} = ma_{p/b} \qquad (3)$$

Where, F_{app} is the horizontal external applied force. If F_{app} and $ma_{b/g}$ are equal and opposite in direction they cancel, giving:

$$F_h = ma_{p/b} \qquad (4)$$

Thus, by adding F_{app} and making it equal to $ma_{b/g}$, the dynamics of the person in the treadmill belt-based frame of reference are equivalent to those describing overground acceleration in a ground-based frame of reference (Eq. 1).

In a simple case where $ma_{p/b}$ is constant, F_{app} needs to be constant and assuming the person can maintain a consistent fore-aft position on the treadmill, can be applied by a tensioned spring element. Therefore in the EA condition, a force equal to body mass multiplied by belt acceleration was generated in a rubber spring element using a winch, and measured via a load cell (Tedea Huntleigh 614,

139 Vishay Precision Group, PA, USA) in series. The rubber spring was attached to the
140 person via a torso harness so that the force was applied close to the body centre
141 of mass. Any fore-aft oscillation of the body during each stride would potentially
142 increase or decrease tension in the tubing. To minimise the effect of oscillations,
143 compliant latex surgical tubing (inner diameter: 3.0 mm, outer diameter: 5.0 mm,
144 Gecko Optical, WA, Australia) was used and stretched from an original length of
145 1.5 m to at least 4.0 m at all accelerations. By using a spring of low stiffness at a
146 large strain, the effects of oscillations of the body on spring tension are
147 minimised (Donelan and Kram, 1997).

148 *Force and work calculations* - The instrumented treadmill has two belts (front and
149 back) with a tri-axial force plate under each. Participants were instructed to
150 walk/run over the join in the belts to maintain a constant fore-aft position on the
151 treadmill. GRF data and the analogue signal from the load cell were sampled at
152 2000 Hz in Qualisys Track Manager software (Qualisys, Sweden). Raw GRF and
153 load cell signals were filtered using a second order bidirectional low-pass
154 Butterworth digital filter at a cut off of 25 Hz. To calculate the net fore-aft
155 impulse generated by GRF (I_{GRF}) in each step, the fore-aft GRF signals from both

force plates were summed and integrated with respect to time from each heel strike to the subsequent contralateral heel strike. Over each step, a theoretical value for I_{GRF} (I_{TH}) was also calculated as:

$$I_{TH} = m\Delta v_{belt} \qquad (5)$$

Where m is the participant's body mass and Δv_{belt} is the change in treadmill belt velocity over that step. This theoretical value represents the net impulse that would have to be generated to cause an equivalent acceleration of the participant overground.

Net external work per step was calculated with an adaptation of the combined limbs method of Donelan et al. (2002). The first step was to calculate net external force by summing the two ground reaction forces and subtracting the spring force measured by the load cell from the horizontal component and subtracting body weight from the vertical component. Net external force was divided by body mass to get COM acceleration and COM acceleration was integrated with time to get COM velocity, setting the initial horizontal velocity to the velocity of the treadmill belt at heel strike. This was performed on each individual step and

instantaneous COM power across each step was calculated as the dot product of COM velocity and the summed GRF. Net external work (W_{COM}) for each step was the time integral of COM power from heel strike to subsequent contralateral heel strike. Theoretical net external work for each step (W_{TH}) was calculated as:

$$W_{TH} = \frac{1}{2}m({v_{fbelt}}^2 - {v_{ibelt}}^2) \qquad (6)$$

Where, m is body mass, v_{fbelt} is the velocity of the belt at the end of the step and v_{ibelt} is the velocity of the belt at the start of the step. This theoretical value represents the net mechanical work that would have to be generated to cause an equivalent acceleration of the participant overground.

Data reduction & statistics - To test our first hypothesis, we compared I_{GRF} with I_{TH} and W_{COM} with W_{TH} for TT and EA conditions, using linear regressions generated in Matlab™ (The Mathworks, MA, USA) software, including all steps during the acceleration phase of trials from all participants in the two conditions. A slope close to one and an intercept of zero would indicate that the experimental condition induced work and impulse values similar to theoretical calculations. To reduce the data for subsequent analyses of GRF data, steps

where either I_{GRF} or W_{COM} were more than ±10% of their theoretical equivalents and steps where the load cell force was more than ±10% of mass multiplied by belt acceleration were removed. Thus, further analyses only analysed EA steps that had whole-body dynamics similar to overground accelerations. Furthermore, the walk-run transition step and any surrounding steps that exhibited atypical GRF profiles (as assessed qualitatively by visual inspection) were removed. A final potential issue was that deformation of the treadmill belt or friction induced by the participants weight force needed to be overcome by the treadmill motor to maintain belt acceleration and power flow between the belt and the participant (Van Ingen Schenau, 1980). To check this, belt velocity was recorded from the treadmill's inbuilt rotary encoder on its roller and average acceleration over each step was calculated and checked to be within ±10% of the required value.

To test the second hypothesis, a number of metrics related to GRF were determined. Maximum braking (most negative) and propulsive (most positive) horizontal GRF values were determined for each stance phase. We also computed the peak and mean two-dimensional sagittal plane magnitude of the GRF vector and the median two-dimensional sagittal plane orientation of the GRF vector

205 (relative to vertical) for each stance phase. For walking, this orientation was
206 calculated for the GRF vector under the foot of the limb that was initially leading.
207 A custom Matlab™ (The Mathworks, MA, USA) algorithm was used to compute
208 right and left limb GRF vectors, by combining the front and rear force vectors
209 and computing the resultant point of application at times when the foot
210 contacted both plates. To examine temporal characteristics, step and stance times
211 were calculated from GRF data.

212 GRF and temporal data were reduced to group means (± s.d.) that were
213 calculated from individual participant means at each acceleration (A0 was treated
214 as zero acceleration). We analysed the effect of acceleration on GRF and temporal
215 metrics with multiple linear regression analyses. Predictor variables were always
216 acceleration and belt velocity, to elicit any effects of acceleration independently
217 of any confounding influence of velocity, which affects step length, step rate,
218 contact time and GRF magnitude and orientation (McMahon and Cheng, 1990).
219 Regression analyses were performed in Matlab™ (The Mathworks, MA, USA) using
220 the '*fitlm*' function on individual participant data and the median of all
221 participants' p-values for the coefficient related to acceleration was computed. If

222 the median p-value was less than 0.05 then acceleration was considered to have
223 a significant effect on that dependent variable.

224 *Results*

225 *Comparison to theoretical data* - For the EA condition, the average force applied
226 by the rubber tubing over a step is shown for each participant, at each
227 acceleration in Figure 2. The application of horizontal force in the EA condition
228 resulted in a significant ($P < 0.001$) linear fit between W_{TH} and W_{COM} with a slope
229 of 1.19 and adjusted R^2 of 0.41, whereas the fit for the TT condition had a non-
230 significant ($P = 0.29$) slope of 0.06 and adjusted R^2 less than 0.01 (Figure 3a).
231 Similarly, fits between I_{TH} and I_{GRF} had slopes of 0.95 ($P < 0.001$, $R^2 = 0.3$) and
232 0.10 ($P = 0.06$, $R^2 = 0.01$) for the EA and TT conditions, respectively.

233 *Effects of emulated acceleration* - Regression analyses revealed a significant effect
234 of acceleration on the two-dimensional orientation of the median GRF vector
235 during the stance phase of walking (Table 1, $P = 0.001$) and running (Table 1, $P =$
236 0.0006). The effect was that increasing acceleration from zero in the A0 condition
237 to 0.76 $m \cdot s^{-2}$ in A3 caused a progressive rotation of the median GRF vector (3.2 ±

238 1.1° for walking and 3.5 ± 2.1° for running) that oriented the vector more
239 anteriorly. This equates to rotations of 4.2° (walking) and 4.6° (running) per 1 $m \cdot s^{-2}$
240 increment in acceleration. Exemplar plots of GRF data exhibiting this rotation for
241 one participant are shown in Figure 4 and data for each participant are available
242 in the supplementary information (Figures S1 and S2). There was no difference
243 found in the mean or peak magnitude of the two-dimensional GRF vector during
244 running but the peak magnitude for walking increased with acceleration (Table 1).
245 There was a significant effect of acceleration on peak braking and propulsive
246 horizontal GRF values with peak braking GRF generally decreasing across
247 conditions from A0 to A3 (walking: $P = 0.04$; running: $P < 0.001$) and peak
248 propulsive GRF increasing for walking and running (walking: $P = 0.02$; running: P
249 $= 0.01$, Table 1). Step time and stance time both decreased with acceleration
250 during walking ($P < 0.01$) but neither changed with acceleration for running steps
251 (Table 1).

252 *Discussion*

253 *Emulated acceleration vs. typical treadmill locomotion* - The first aim of this study
254 was to show if providing an external force to compensate for inertial forces
255 during locomotion on an accelerating treadmill belt could elicit mechanics more
256 similar to true accelerations than typical treadmill locomotion. The main criteria
257 for this were that W_{COM} and I_{GRF} were more similar to their theoretical
258 counterparts (W_{TH} and I_{TH}) in the EA condition than in the TT condition. If EA
259 induced net work and GRF impulse identical to theoretical values than the linear
260 fits for EA in Figure 3 should be represented by the equation $y = x$. As can be
261 seen from the linear fit in Figure 3A, net positive work increased with increasing
262 belt acceleration for EA but the coefficients of the fit indicated that
263 experimentally determined net work generally exceeded the values derived from
264 theoretical calculations. The same was found for the fit between I_{GRF} and I_{TH},
265 although the slope for this fit was closer to one (0.95). Although, data from the
266 EA condition generally resulted in greater work and impulse than desired, as
267 hypothesised it did induce mechanics far closer to theoretical values than the TT
268 condition. The slopes of linear fits to TT data in Figure 3 showed that W_{COM} and
269 I_{GRF} barely changed at all with increasing theoretical values that explained virtually

none of the variance in the experimental data. This reinforces previous work by Van Caekenberghe and colleagues (2013b) that showed mean propulsive GRF and propulsive GRF impulse (normalised to body mass) was significantly less for running on an accelerating treadmill belt when compared to GRF during equivalent acceleration overground. The current data show that even by using a relatively simple, low-tech method to compensate for inertial forces when on an accelerating treadmill belt, mechanical demands match much more closely what the real demand of accelerating the body should be. As will be discussed later, more high-tech solutions may provide a better match, but the current approach can still provide useful data for experimental studies of accelerative locomotion. So as to only analyse data from steps where the mechanical demand closely matched theoretical demands of overground acceleration, further analysis was only conducted on steps where the average compensatory force, W_{COM} and I_{GRF} were within ±10% of the corresponding theoretical value for that step. This provided a total of 173 steps (across all participants) from the EA condition for analysis of acceleration mechanics. The total number of steps before reduction was 874, meaning only 20% of all potential steps met the inclusion criteria.

287 Furthermore, for walking steps four participants had no steps that met the criteria
288 for at least one of the belt accelerations. Thus, the walking data set consisted of
289 only five participants' data.

290 *The effects of emulated acceleration* - Previous work has examined overground
291 how GRF data and temporal metrics change with increasing acceleration during
292 running (Kugler and Janshen, 2010; Van Caekenberghe et al., 2013a). The second
293 aim of the present study was to test if similar adaptations occur for emulated
294 acceleration. Van Caekenberghe et al. (2013a) identified that the GRF vector
295 rotated 4° anteriorly for every 1 $m \cdot s^{-2}$ increment in acceleration. Our EA condition
296 resulted in a similar 4.6° rotation per 1 $m \cdot s^{-2}$ during running. We observed that
297 the rotation of the GRF vector occurred with no change in the mean magnitude
298 of the GRF vector. This indicated that the increase in net positive horizontal
299 impulse that occurred with acceleration was achieved via reorientation of the GRF
300 vector, rather than an increased total GRF. This finding is also consistent with
301 previous observations for overground accelerations (Kugler and Janshen, 2010;
302 Van Caekenberghe et al., 2013a). Furthermore, Van Caekenberghe et al. (2013a)
303 showed very small reductions in step duration and no change in stance duration

304 to occur with increasing acceleration for running and we have found a similar
305 result for EA. Therefore, in terms of kinetics and temporal measures, our
306 emulated acceleration setup elicited similar strategies for increasing acceleration
307 during running as are employed overground.

308 *Limitations & potential applications* - A low-tech approach was employed to
309 applying the appropriate compensatory force to participants and this led to some
310 limitations. First, the tension in the elastic tubing had to be set manually using a
311 winch and real-time feedback viewed on a computer monitor, prior to the
312 commencement of walking. The precision of this approach is somewhat limited
313 and, as can be seen in Figure 2, appropriate forces were not always applied. This
314 might explain some of the RMS errors (17.4 J and 8.3 N) in the linear regression
315 models for work and impulse data before steps with inappropriate compensatory
316 force were removed (Figure 3). The approach also meant that the compensatory
317 force could not be adjusted on the fly and thus it was only possible to emulate
318 constant acceleration rather than a varied acceleration profile. Any significant
319 fore-aft variation in the participants' position on the treadmill would cause
320 fluctuations in the tension in the elastic tubing and potentially result in

inappropriate compensatory force. The effect of this was minimised by using compliant tubing operating at high strain (Donelan and Kram, 1997) and ultimately, steps with inappropriate force were removed from further analysis. The approach provided sufficient valid steps for analysing acceleration mechanics but the number of steps that did not closely mimic real acceleration and the inability to vary acceleration on the fly mean that it would not be an appropriate setup for situations that require full simulation of gait, such as treadmill-based gait rehabilitation. For these scenarios, a more high-tech solution incorporating force-feedback and real-time control (Christensen et al., 2000; Hidler et al., 2011) might be more effective.

Conclusions - The limitations of the simple setup employed here to apply a compensatory force may make it inappropriate for use as a rehabilitation tool for simulating acceleration, as many steps do not have mechanics similar to real accelerations. For the same reason, it also does not allow for significantly more steps of data to be collected than overground experimental setups. However, it did permit sufficient steps of appropriate data to be collected for investigations into the mechanics and muscular strategies used for accelerating the body. This is

extremely useful as the treadmill environment facilitates the use of wired data collection systems and smaller lab spaces for such experiments. This study also showed that if appropriate external mechanics are attained, they are attained through the same adjustments in GRF and temporal characteristics as have been observed for overground accelerations. Therefore, the technique used is suitable for investigations of acceleration strategies during locomotion and more precise systems for applying compensatory force should more effectively emulate real acceleration mechanics.

Acknowledgements

D.J.F. was funded by a post-doctoral fellowship provided by the Australian Sports Commission. This work was also partially internally funded by The University of Queensland. The author would like to acknowledge valuable discussions regarding this work with Dr. Nicholas Brown (Australian Institute of Sport), Dr. Glen Lichtwark (The University of Queensland), Prof. Andrew Cresswell (The University of Queensland) and Dr Greg Sawicki (North Carolina State University).

Conflict of Interest Statement

The author declares no conflict of interest related to this work.

References

Caputo, J.M., Collins, S.H., 2013. An Experimental Robotic Testbed for Accelerated Development of Ankle Prostheses, 2013 Ieee International Conference on Robotics and Automation, pp. 2645-2650.

Christensen, R.R., Hollerbach, J.M., Xu, Y., Meek, S.G., 2000. Inertial-force feedback for the treadport locomotion interface. Presence 9, 1-14.

Donelan, J.M., Kram, R., 1997. The effect of reduced gravity on the kinematics of human walking: A test of the dynamic similarity hypothesis for locomotion. Journal of Experimental Biology 200, 3193-3201.

Donelan, J.M., Kram, R., Kuo, A.D., 2002. Simultaneous positive and negative external mechanical work in human walking. Journal of Biomechanics 35, 117-124.

Goldberg, E.J., Kautz, S.A., Neptune, R.R., 2008. Can treadmill walking be used to assess propulsion generation? Journal of Biomechanics 41, 1805-1808.

Hidler, J., Brennan, D., Black, I., Nichols, D., Brady, K., Nef, T., 2011. ZeroG: overground gait and balance training system. Journal of Rehabilitation Research Development 48, 287-298.

Kugler, F., Janshen, L., 2010. Body position determines propulsive forces in accelerated running. Journal of Biomechanics 43, 343-348.

McMahon, T.A., Cheng, G.C., 1990. The Mechanics of Running - How Does Stiffness Couple with Speed. Journal of Biomechanics 23, 65-78.

Morin, J.B., Samozino, P., Bonnefoy, R., Edouard, P., Belli, A., 2010. Direct measurement of power during one single sprint on treadmill. Journal of Biomechanics 43, 1970-1975.

Peterson, C.L., Kautz, S.A., Neptune, R.R., 2011. Braking and propulsive impulses increase with speed during accelerated and decelerated walking. Gait and Posture 33, 562-567.

Qiao, M., Jindrich, D.L., in press. Leg joint function during walking acceleration and deceleration. Journal of Biomechanics -, -.

Van Caekenberghe, I., Segers, V., Aerts, P., Willems, P., De Clercq, D., 2013a. Joint kinematics and kinetics of overground accelerated running versus running on an accelerated treadmill. Journal of The Royal Society Interface 10, 20130222.

Van Caekenberghe, I., Segers, V., Willems, P., Gosseye, T., Aerts, P., De Clercq, D., 2013b. Mechanics of overground accelerated running vs. running on an accelerated treadmill. Gait and Posture 38, 125-131.

Van Ingen Schenau, G.J., 1980. Some Fundamental Aspects of the Biomechanics of Overground Vs. Treadmill Locomotion. Medicine and Science in Sports and Exercise 12, 257-261.

Figure Captions

Figure1. Schematic illustration of the experimental setup for emulated acceleration. Participants walked and ran over the split in the treadmill belts while wearing a harness attached to a length of rubber tubing. A lockable winch

situated 4 m behind the treadmill was used to tension the rubber tubing and a load cell in series between the tubing and the harness measured the force in the tubing. The rubber tubing and load cell were disconnected from the harness for the typical treadmill locomotion condition.

Figure 2. Participant mean (± s.d.) body mass normalised average compensatory force measured by the load cell. Data are the mean of instantaneous force values over a step. Presented values are the mean of all steps for each participant in the respective acceleration conditions (A1 - light grey, A2 - dark grey, A3 - black). Horizontal dashed lines indicate the target force for each acceleration.

Figure 3. Scatter plots and linear regression fits to theoretical vs. experimentally determined net work (a) and net impulse (b) for emulated acceleration (hexagons, dashed black lines) and typical treadmill locomotion (crosses, solid grey lines). Data points include all steps for all participants walking and running. Acceleration conditions are indicated by the darkness of the data point (light - dark = A1-A3). The coefficients of the linear fits are also shown on each panel.

Figure 4. Exemplar plots of horizontal vs. vertical GRF, normalised to body weight, for running (a) and walking (b) steps. Solid black lines - A0, solid grey lines - A1, dashed grey lines - A2 and dashed black lines - A3. Data are from individual trials at each acceleration, in the EA condition, from one participant. Arrows indicate the direction of the loop from heel strike to toe-off. The clockwise rotation of the median ground reaction force vector that was calculated can qualitatively be observed in this figure by noting that as acceleration increased, the GRF loops shift to predominantly anterior (positive) values for the horizontal component.

Figure 1
Click here to download Figure: Figure1.eps

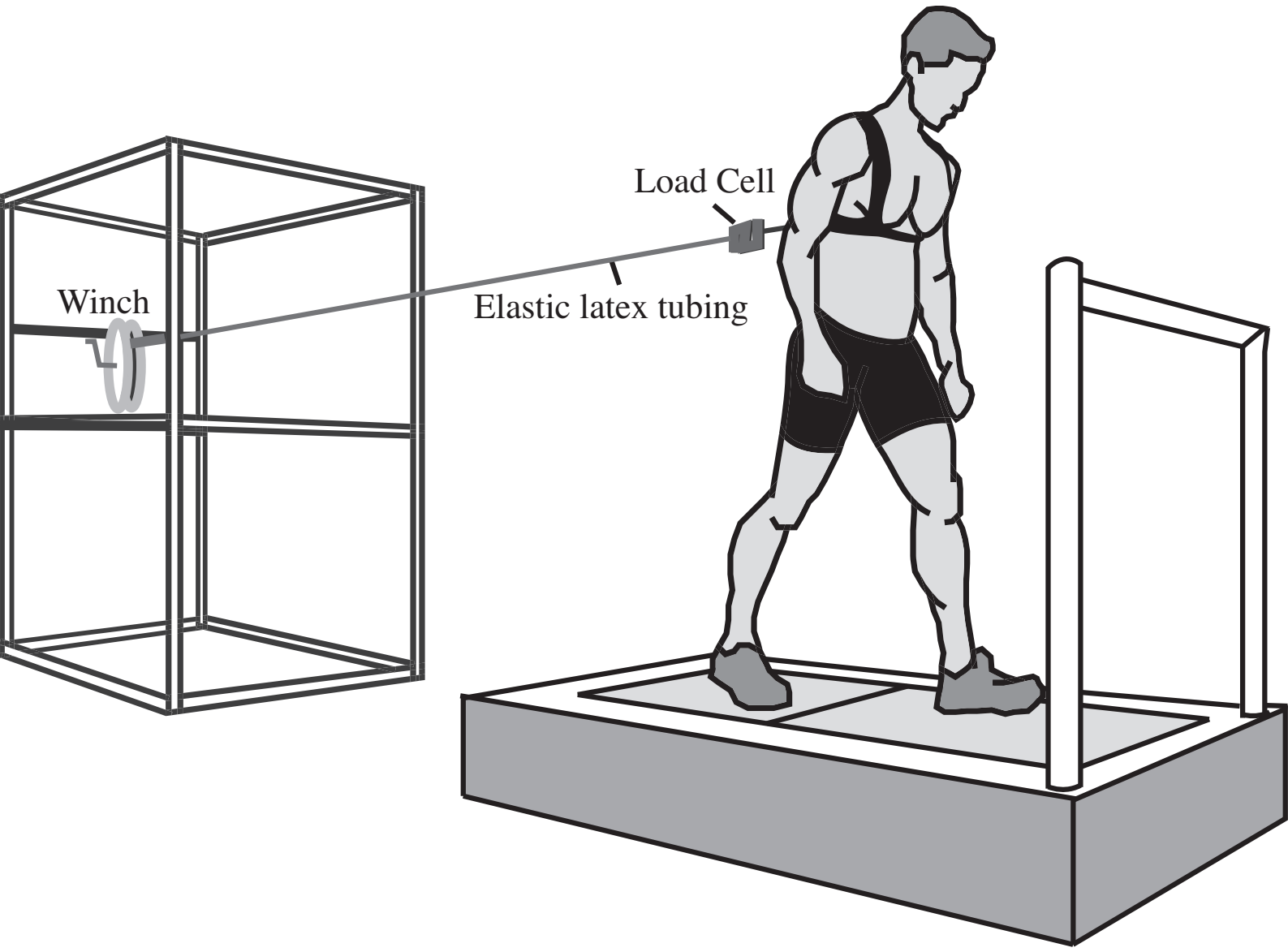

Figure 2
Click here to download Figure: Figure2.eps

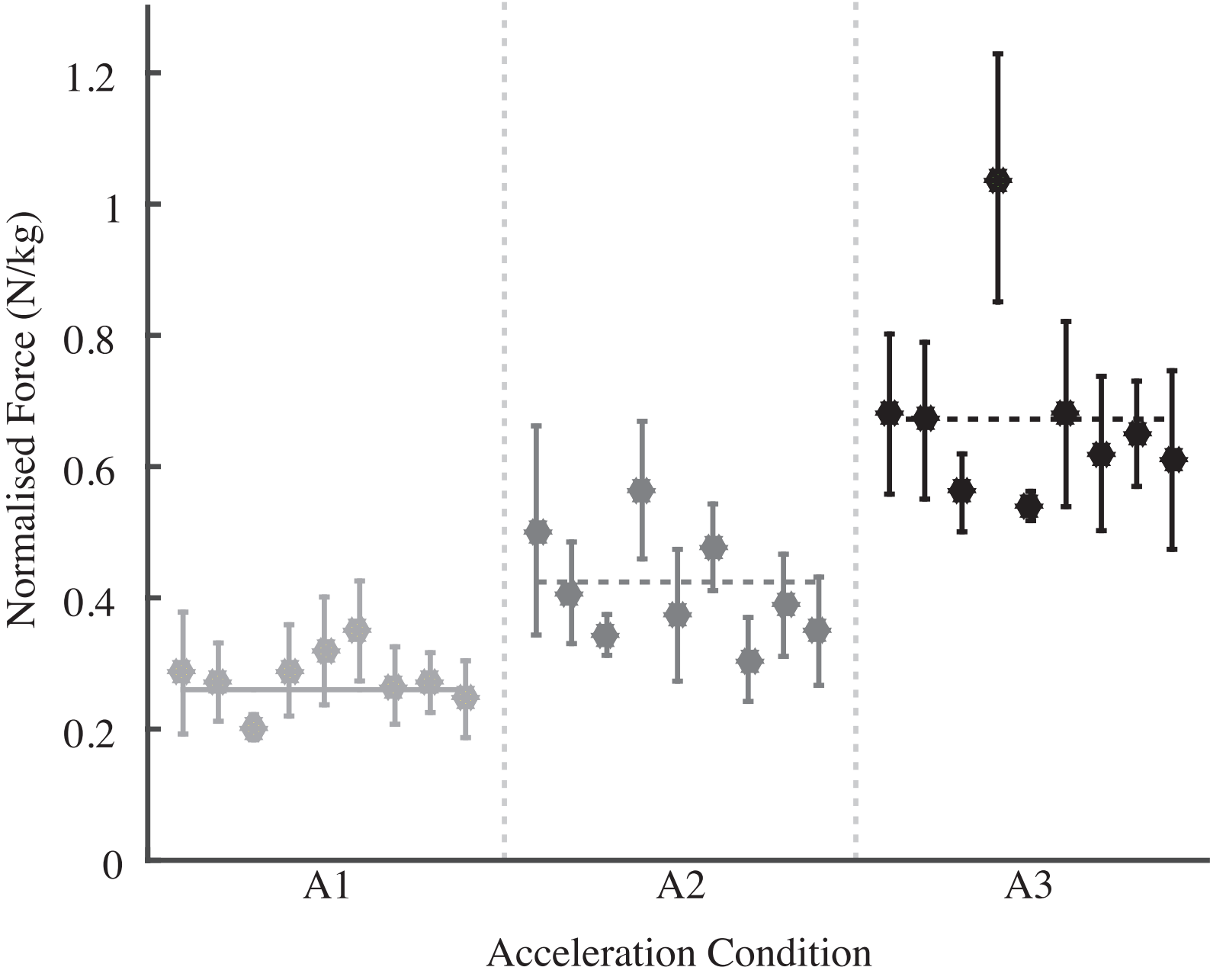

Figure 3
Click here to download Figure: Figure3.eps

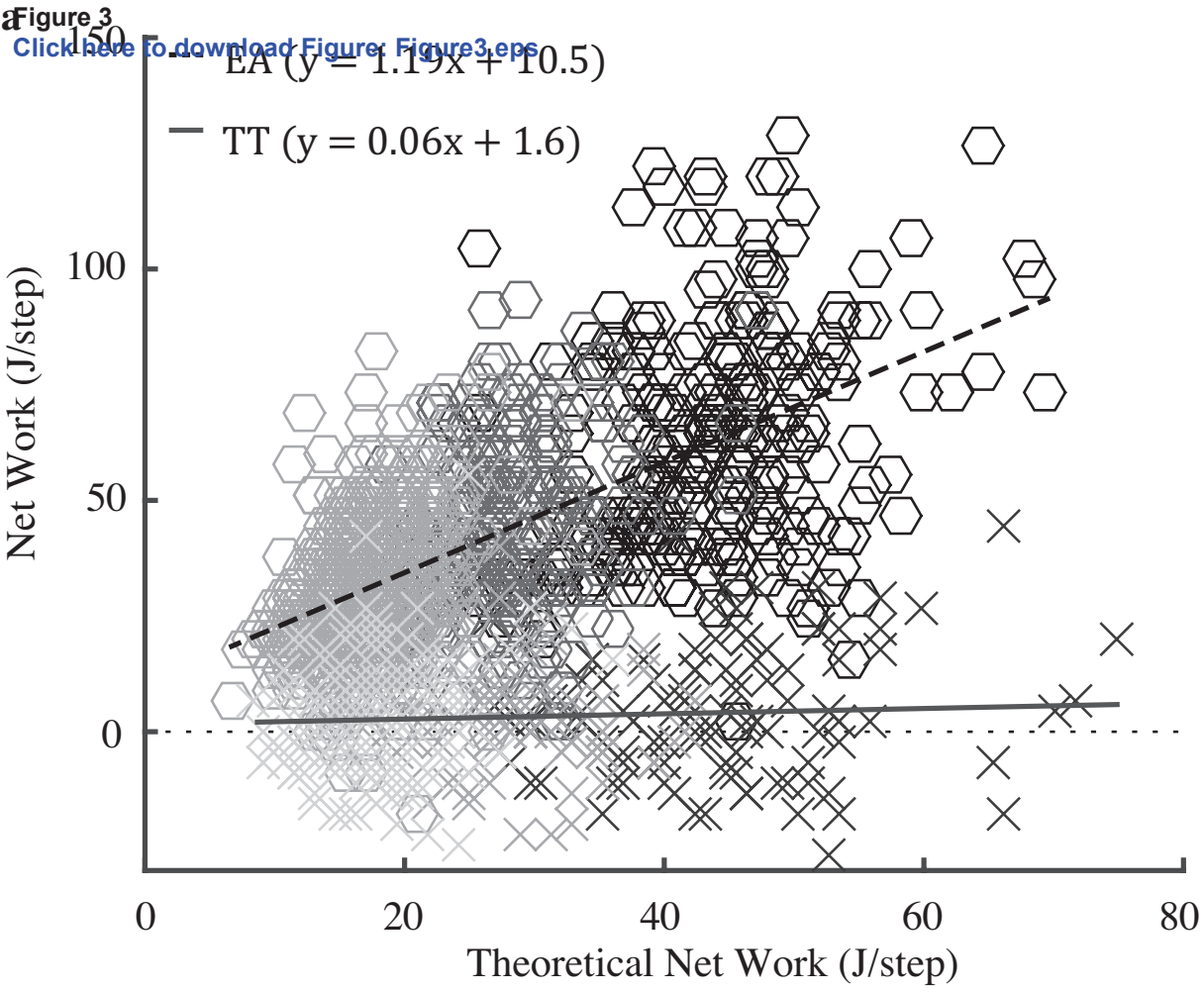

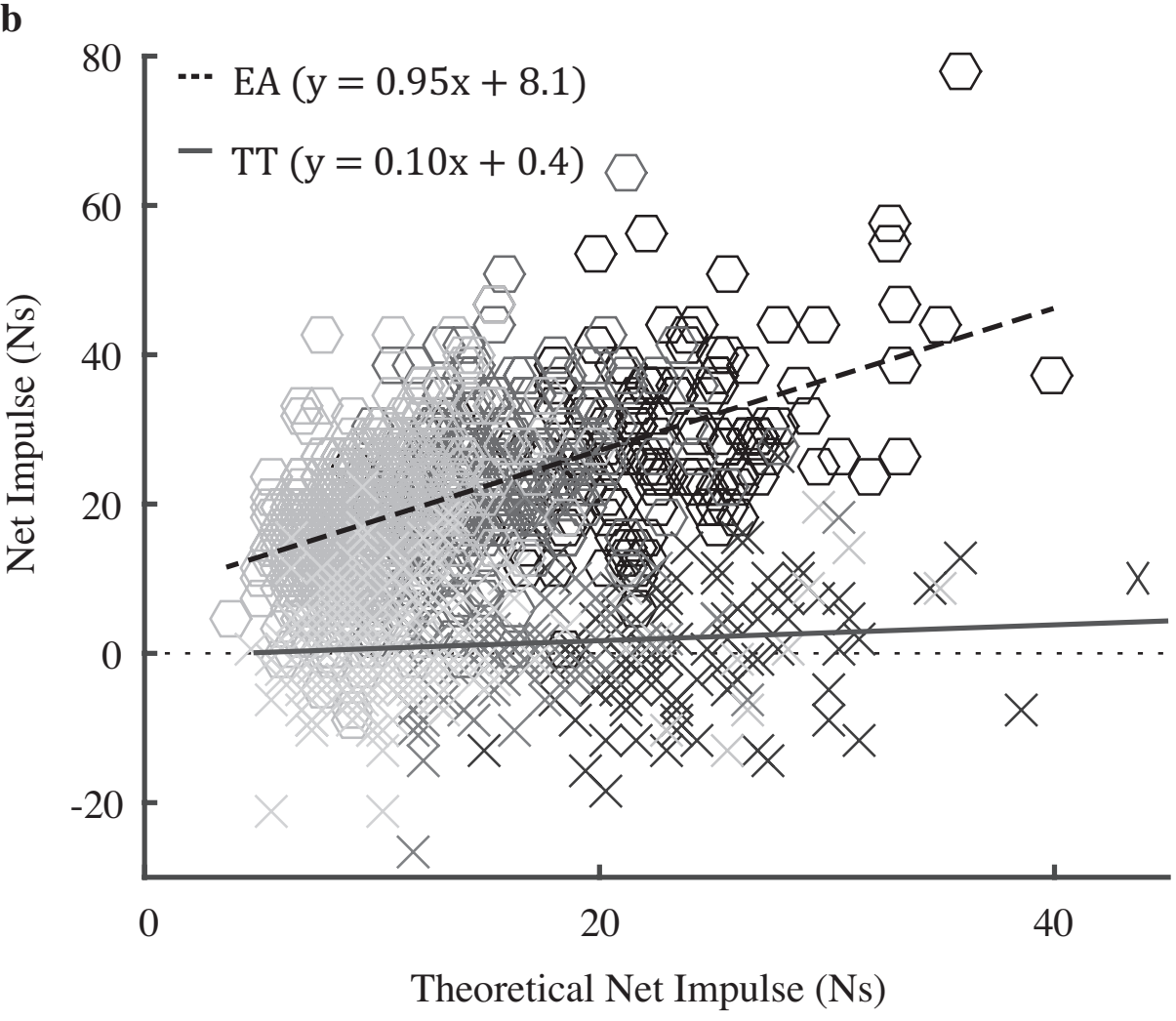

Figure 4
Click here to download Figure: Figure4.eps

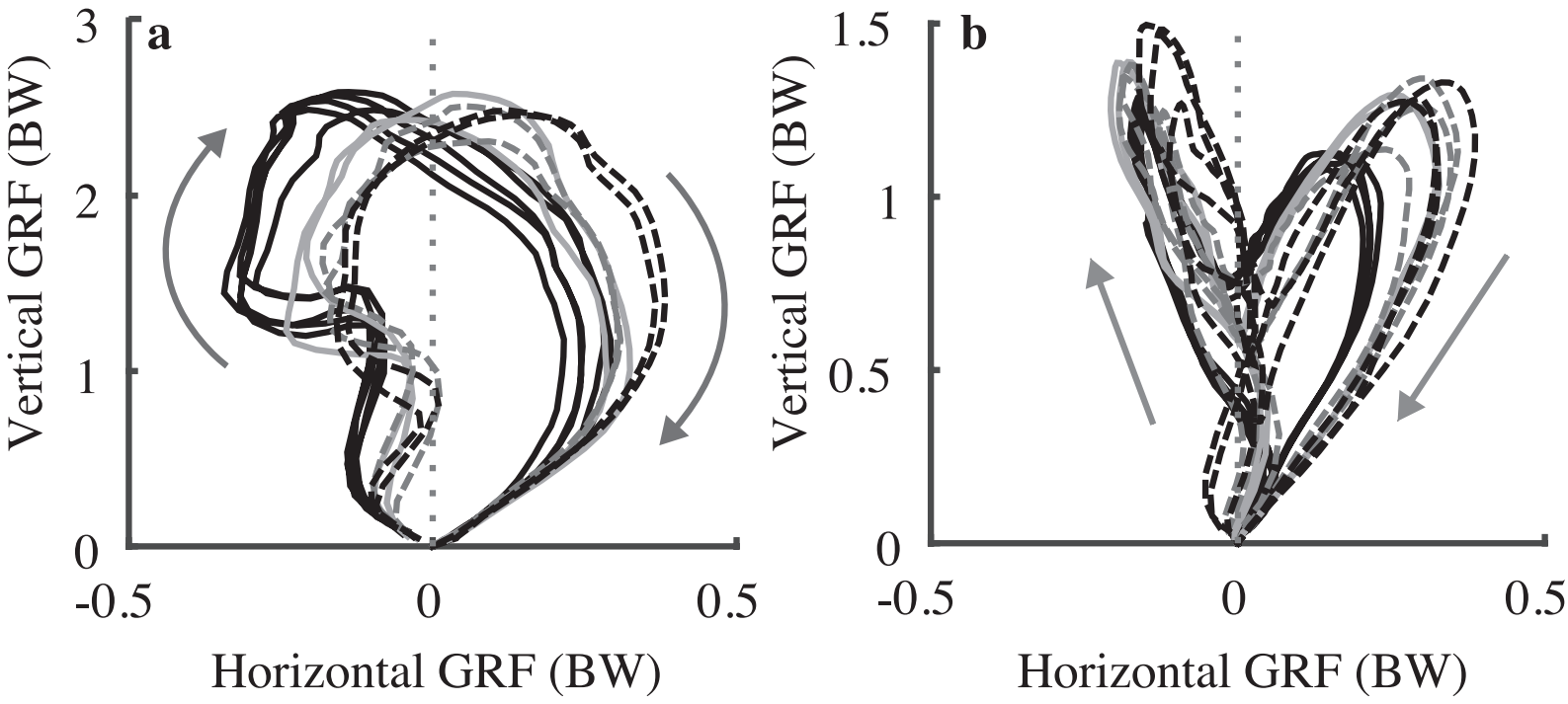

Table

Table1. Summary of group mean ± standard deviation GRF and temporal metrics

	Walking				Running			
Acceleration ($m \cdot s^{-2}$)	0	0.27	0.42	0.76	0	0.27	0.42	0.76
Peak braking GRF (N) *#	-133 ± 9	-143 ± 23	-140 ± 20	-103 ± 11	-195 ± 29	-151 ± 29	-148 ± 27	-114 ± 30
Peak propulsive GRF (N) *#	162 ± 20	225 ± 33	253 ± 21	237 ± 29	206 ± 39	224 ± 49	240 ± 39	260 ± 55
Peak GRF magnitude (N) *	895 ± 76	988 ± 54	962 ± 54	1040 ± 95	1947 ± 254	1794 ± 236	1832 ± 234	1859 ± 272
Mean GRF magnitude (N)	630 ± 52	657 ± 34	655 ± 47	637 ± 23	1052 ± 154	986 ± 126	996 ± 117	1027 ± 138
Median GRF vector orientation (°) *#	0.1 ± 1.2	1.5 ± 1.0	2.4 ± 0.9	3.3 ± 1.1	0.7 ± 1.1	2.2 ± 1.1	3.3 ± 1.7	4.2 ± 1.6
Step time (s) *	0.585 ± 0.029	0.549 ± 0.056	0.558 ± 0.070	0.486 ± 0.016	0.392 ± 0.022	0.392 ± 0.034	0.395 ± 0.026	0.375 ± 0.020
Stance time (s)	-	-	-	-	0.304 ± 0.026	0.330 ± 0.022	0.321 ± 0.036	0.303 ± 0.032

*Denotes a significant effect of acceleration for walking steps and # indicates a significant effect of acceleration for running steps

Figure S1

Click here to download Supplementary Material: FigureS1_running.pdf

Figure S2

Click here to download Supplementary Material: FigureS2.pdf

Conflict of Interest Statement

The author declares no conflict of interest related to this work.